Geometrical-Based Throughput Analysis of Device-to-Device Communications in a Sector-Partitioned Cell

Minming Ni, *Member, IEEE*, Jianping Pan, *Senior Member, IEEE*, and Lin Cai, *Senior Member, IEEE*

***Abstract*—Device-to-device (D2D) communications in cellular networks are considered a promising technology for improving network throughput, spectrum efficiency, and transmission delay. In this paper, the Power Emission Density (PED)-based interference modeling method is applied to explore proper network settings for enabling multiple concurrent D2D pairs in a sector-partitioned cell. With the constraint of the Signal-to-Interference Ratio (SIR) requirements for both the macro-cell and D2D communications, an exclusive region-based analytical model is proposed to obtain the guard distances from a D2D user to the base station, to the transmitting cellular user, and to other communicating D2D pairs, respectively, when the uplink resource is reused. With these guard distances, the bounds of the maximum throughput improvement provided by D2D communications are then derived for different sector-based resource allocation schemes. Extensive simulations are conducted to verify our analytical results. The new results obtained in this work can provide useful guidelines for the deployment of future cellular networks with underlaying D2D communications.**

***Index Terms*—Device-to-device communications, uplink resource reusing, interference analysis, throughput bound.**

I. Introduction

By taking advantage of the proximity between network nodes, device-to-device (D2D) communications in cellular networks are expected to improve network performance in several aspects. With D2D communications, the data exchanges between nearby user equipments (UEs) could be finished through direct radio links, rather than being relayed via the centralized base station (BS). Due to this short distance characteristic, D2D communications not only decrease the transmission delay effectively, but also relax the requirement of transmission power for successful reception, which greatly increases the energy efficiency. More importantly, D2D communications in cellular networks bring a great chance to boost network throughput and enhance spectrum efficiency by reusing the radio resources originally allocated to the cellular UEs (CUEs). In light of all these potential advantages, the D2D communications are recognized as one of the key components in the next-generation cellular networks to satisfy the increasing demand on high data-rate wireless access services.

Among all the challenges for enabling D2D communications in cellular networks, the possible interference generated by spectrum sharing is of high priority. For example, a CUE's uplink transmission might cause a great impact on the nearby D2D communication, which is reusing the same wireless resource. Furthermore, if there are multiple concurrently transmitting D2D pairs, the accumulated interference may also influence the quality of the intended uplink signal received at the BS. Similarly, when the downlink resources are reused by D2D UEs (DUEs), their transmissions might also cause the reception failures of CUEs nearby. In view of this inevitable issue, various research work had been finished specifically for the interference management of D2D communications in cellular networks. However, most of these work only investigated a relatively simple scenario that the resource blocks allocated to a CUE are only reused by one D2D pair within the same cell. Although this *Single-Reusing* scenario is easy to be implemented, it still leaves a great space to further improve the resource efficiency, especially when the D2D communication's short distance characteristic is considered.

To fill the gap, we had already studied the *Multi-Reusing* scenario, in which multiple D2D pairs are enabled to communicate concurrently by reusing the identical uplink resources within the same cell, in our previous work [1]. With the consideration of Signal-to-Interference Ratio (SIR) requirements for both the uplink cellular and D2D transmissions, a geometrical method was used to obtain the guard distances from a DUE to the BS, to the transmitting CUE, and to the other communicating DUEs. With these guard distances, successful receptions at the DUE receivers and the BS could be guaranteed, and the throughput bounds were finally derived. However, the interference analyses accomplished in [1] still followed the traditional *discrete-style* method, in which the accumulated interference power measured at a reference point y can be generally presented as [2]

$$I_{\mathrm{ACC}}(y) = \sum_{x \in \mathcal{A}} P_x h_x L(\|y - x\|), \tag{1}$$

where $\mathcal{A}$ denotes the set of all the transmitting nodes, P_x is the transmission power of node x, h_x is the channel fading

Manuscript received June 15, 2014; revised November 21, 2014; accepted December 5, 2014. Date of publication December 18, 2014; date of current version April 7, 2015. This work is partly supported by the NSFC (Grant No. 61401016), State Key Laboratory of Rail Traffic Control and Safety (Grant No. RCS2014ZT33, RCS2014ZQ003, and RCS2012ZT007), the Fundamental Research Funds for the Central Universities (Grant No. 2014JBM154), NSERC (with contributions from DRDC), CFI, and BCKDF. The associate editor coordinating the review of this paper and approving it for publication was S. Mao.

M. Ni was with the University of Victoria, Victoria, BC V8P 5C2, Canada. He is now with the State Key Laboratory of Rail Traffic Control and Safety, Beijing Jiatong University, Beijing 100044, China (e-mail: mmni@bjtu.edu.cn).

J. Pan is with the Department of Computer Science, University of Victoria, Victoria, BC V8W 2Y2, Canada (e-mail: pan@uvic.ca).

L. Cai is with the Department of Electrical and Computer Engineering, University of Victoria, Victoria, BC V8W 2Y2, Canada (e-mail: cai@ece.uvic.ca).

Digital Object Identifier 10.1109/TWC.2014.2382639

coefficient, and $L(\cdot)$ is the path-loss function, assuming to depend only on the distance $\|y-x\|$ from node x to the reference point y. However, for the D2D communication scenario, due to the fact that the network area left for simultaneous communicating D2D pairs is usually a finite irregular region determined by both the BS and the active CUEs, neither $\mathcal{A}$ nor $\|y-x\|$ is easy to be accurately obtained. Therefore, some approximations were made in [1], but they might be inapplicable to the more generalized scenarios, such as when the observed cell area is divided into multiple sectors.

Rather than following the existing approaches, in this paper, we investigated the multi-reusing scenario from a new angle. By applying our recently proposed Power Emission Density (PED)-based interference modeling method [3], the interference power accumulated at the BS and the receiving DUEs can be obtained easily by a *continuous-style* analysis, which does not require the information of either the concurrent transmitter set or interference transmission distance mentioned in (1). Therefore, a series of approximations and assumptions used in [1], e.g., ignoring the difference of the path-loss exponents between CUE-BS and D2D links, and constant bit rate D2D communication, are removed in this work for obtaining more general system settings for the multi-reusing scenario. Moreover, due to the fact that the PED-based method has no constraint of the network area's shape, we are now able to study the impact of different resource allocation schemes on the bound performance of D2D communications in a sector-partitioned cell, which is more realistic and meaningful.

To sum up, the main contributions of this paper are twofold. First, we provide the first systematic study of the throughput improvement provided by D2D communications when the cell area is divided into multiple sectors, in which multiple D2D communication pairs are concurrently reusing the cellular uplink resources. Second, this work is also the first practical application of the PED-based interference analysis method, which is proved to have good accuracy, and easy to be utilized for solving some problems that are otherwise cannot be handled by the traditional discrete-style method.

The remainder of the paper is organized as follows. In Section II, we summarized the related work in radio resource allocation and bound performance analysis for D2D communications. After that, The basic idea and main features of the PED-based interference modeling method are explained in Section III. The system model for our analysis is described in Section IV. Subsequently, the guard distances are derived in Section V, and followed by the bound performance analysis of the sector-partitioned cell for all the possible resource allocation cases in Section VI. All the analytical results are verified by simulations in Section VII. Additionally, the possibility for applying the PED-based method to the sparse network scenario, and for introducing the impact of channel fading to further evolve the PED-based method are also briefly discussed in Section VIII. Section IX concludes this paper.

II. Related Work

To control/coordinate the interference and improve the throughput of D2D communications, existing work in the literature can be roughly classified into two categories, including radio resource allocation and theoretical analysis of the performance bounds.

For the radio resource allocation, the initial framework for D2D communications in cellular networks was proposed in [4], which became one of the foundations for the follow-on work on this topic. By assuming that the radio resource managements were adopted for both the cellular and D2D connections, the three widely adopted resource allocation patterns, i.e., non-orthogonal, orthogonal, and cellular operation, were first studied in [5]. After that, various kinds of resource allocation schemes were proposed for achieving different design targets. For example, to alleviate the interference generated from the cellular and D2D communications in the neighboring cells, a resource allocation scheme was proposed in [6] to manage the different frequency bands utilized by DUEs and CUEs according to whether the UEs were located in the inner or outer region of a cell. In [7], the issues of resource allocation and power control were jointly handled to maximize the spectrum utilization by finding the minimum transmission distance for D2D links, while also protecting the CUEs from harmful interference and guaranteeing the quality of service (QoS) for D2D links. In one of the most recent work [8], the resource allocation issue in D2D communications was systematically described in the scope of game theory, and a series of key open research directions were also outlined. Generally, most of the existing resource management schemes focus on the scenario that the resource block allocated to a CUE is only reused by one D2D pair. In other words, the proper design guidelines for supporting multiple concurrent D2D pairs with identical radio resources in the same cell, which is more spectrum efficient, are still unclear for the radio resource allocation schemes.

For the theoretical analysis of performance bounds provided by the D2D communications in cellular networks, available results are relatively fewer. For example, when a D2D communication is enabled in a FDD CDMA-based cellular cell, the uplink capacity gain was derived in [9]. In [10], a lower bound of the ergodic capacity was obtained for uplink radio resource reusing by analyzing the coverage of interference-limited area (ILA), which was used to manage the interference from CUEs to a D2D transaction when multiple antennas were used by the BS. By applying results from stochastic geometry, the maximum achievable transmission capacity, which was defined as the spatial density of successful transmissions per unit area, was analyzed for the hybrid D2D and cellular network in [11]. However, identical to the existing issues in the radio resource allocation, due to the inevitable interference accumulated at the BS, most of the existing analytical results obtained by assuming that a single D2D pair in a cellular network cannot be directly extended to a scenario with multiple simultaneously communicating D2D pairs. Meanwhile, similar performance studies have also been conducted in the heterogeneous and cognitive network scenarios. For example, to obtain the maximum per-user throughput, a user-centric WiFi-offloading model was proposed for the heterogeneous network in [12], which shares the idea of utilizing users' proximity with D2D communications in cellular networks. In [13], a new system model was used to study the coexistence between machine-to-machine communications and

human-to-human communications in the same network, which further formulated a non-transferable utility coalition game to study the performance of both the direct and relay transmissions. Unfortunately, the new models and methods applied in these works still cannot effectively solve the problems in the multi-reusing D2D communication scenarios.

III. PED-Based Interference Modeling Method

In the wireless networks, due to the broadcast nature of the wireless transmission, each communicating node pair has to solely occupy a part of the network area, which is usually refereed to as the *Exclusive Region* (ER) [14], for guaranteeing their transmission quality. Therefore, it is possible for us to borrow the idea of "Area-Point" equivalence, which is widely used in astrophysics and thermodynamics for simplifying the related theoretical analyses[1], to equalize the interference effect generated by the actual *point transmitter* to the one produced by an imagined *area transmitter*. Moreover, the imagined area transmitter can be designed to occupy the same network area of the tagged point transmitter's ER, so the non-overlapping feature of the concurrent ERs can also be utilized. Combining with the fact that, when the network is densely deployed, the network area can be approximated by the sum of all the concurrent ERs. Hence, the accumulated interference at an observed receiver $\mathbf{x}$ under this extreme situation could be represented as an area integral as

$$I_{\mathrm{ACC}}(y) = \int\limits_{\mathcal{S}_{\mathrm{N}}-\mathcal{S}_{\mathrm{E}}} \lambda h_{\mathrm{d}S} L(\|\mathrm{d}S-\mathbf{x}\|)\,\mathrm{d}S, \tag{2}$$

where $\mathcal{S}_{\mathrm{N}}$ is the network area, $\mathcal{S}_{\mathrm{E}}$ is the part of the network area occupied by the observed receiver y and its transmitter as their ER, $\mathrm{d}S$ is the area element for the integral, and λ is the equivalent Power Emission Density (PED) when the transmission power, ER area $\mathcal{S}_{\mathrm{E}}$, and propagation scenario are given. More detailed descriptions for the calculation of PED λ and the PED-based interference analysis method could be found in [3]. By utilizing this *continuous-style* analysis method, the complexity of interference modeling in the random networks could be effectively reduced, while a certain degree of accuracy can still be maintained. Especially, for network nodes deployed within an irregular area, this new method could avoid the complicated (or even infeasible) calculation of transmitting node set $\mathcal{A}$ and transmission distances $\|y-x\|$ in (1). Therefore, the PED-based modeling method could be a useful tool for analyzing the interference-based performance bounds of D2D communications in more general network scenarios.

IV. System Model

For a tractable yet reasonable analysis, the observed cell's coverage area is modeled as a disk with radius r. The directional antennas are assumed to be deployed at the BS for evenly dividing the cell area into n_{S} sectors. In consideration of the modeling complexity, the effect of the directional antennas' side and back lobes is ignored in our analysis, which is common in the literature. According to the different transmission requirements and interference situations, each UE in the network could dynamically switch its working mode between CUE and DUE. In the CUE mode, the UE's data transmissions rely on the BS's forwarding; while in the DUE mode, two UEs establish a direct link to accomplish their data exchange by reusing the uplink radio resources allocated to the cell.[2] Due to the physical features of directional antennas, only part of the accumulated interference power, which is generated by all the D2D communications utilizing the same uplink spectrum within the observed cell, will have the substantial negative impact on a sector's uplink reception. Therefore, the sector-partitioned cell structure should be able to further boost the total throughput improvement provided by the D2D communications. Additionally, all UEs' locations are assumed to be static in the analysis, which is due to the fact that, the mobility during a few packet transmissions (tens of milliseconds) will not affect the distance relationship between network nodes substantially.

A general path-loss model is applied in this paper to describe a signal's power attenuation with the transmission distance as $P_{\mathrm{r}} = \beta P_{\mathrm{t}}/d^{\alpha}$ with $\alpha > 2$, where P_{t} is the transmission power, P_{r} is the average signal power received at distance d from the transmitter, β is a constant determined by the hardware features of the transceivers, and α is the path-loss exponent depending on the propagation environment [16]. Moreover, two parameter sets $(\alpha_{\mathrm{B}}, \beta_{\mathrm{B}})$ and $(\alpha_{\mathrm{D}}, \beta_{\mathrm{D}})$ are used to distinguish the different channel characteristics between the BS-CUE link and the D2D link, respectively. Considering that the DUE and CUE are just two different working modes of UE, the impact of a transmitting CUE on a DUE receiver will also be calculated with the parameter set $(\alpha_{\mathrm{D}}, \beta_{\mathrm{D}})$.

As a consequence of the limited coordinations between the DUE pairs in the network, D2D communications usually use fixed transmission power $P_{\mathrm{t,D}}$, and follow a semi ad-hoc style, especially when multiple concurrent D2D pairs are reusing the same spectrum for their data transmissions respectively. For this paper, while the BS will assist each DUE to determine the proper radio resource for their possible direct transmissions, the DUEs are still assumed to work with the classic Carrier Sense Multiple Access (CSMA) MAC protocol, which means that a DUE transmitter will monitor the state of its allocated channel before initializing its transmission. If the sensed power level is higher than a threshold P_{th}, which is usually one of the basic information for system design, the channel is regarded as busy, and the transmission will be postponed. Due to this sensing process, each transmitting DUE will occupy a minimum area, which is usually termed as the Exclusive Region (ER) [17]. For simplicity, we assume that the ER is a circle with radius G_{D}, and the minimum distance between two concurrent transmitting

[1] For example, the Shell Theorem says that, a spherically symmetric body affects external objects gravitationally as though all of its mass were concentrated at a point at its center [15].

[2] Although some existing work assumes that the D2D communications could be finished by utilizing some unlicensed frequency bands, such as the 2.4 GHz Industrial, Scientific and Medical (ISM) spectrum, considering the fact that the quality of service (QoS) in these bands may fail to be controlled or guaranteed, only the underlaying D2D communications are investigated in this paper. However, with the same method, the analysis can be easily extended to the unlicensed spectrum reusing scenario.

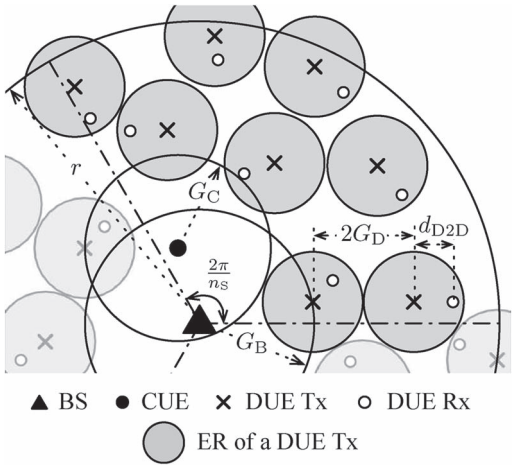

Fig. 1. System model for the D2D communications within a sector-partitioned cell, when $n_S = 3$.

DUEs is $2G_D$ as shown in Fig. 1. It is worth to mention that, when the channel fading is considered, a communicating node pair's ER will became an irregular region, which is much more complicated. We will keep using the simplified disk model in the following part of this paper, but also working on the more realistic interference model as the follow-on studies. A brief discussion about our recent progress on this topic is given at the end of this paper. Besides the consideration of ERs, we also define that a D2D connection will only be established when the distance d_{D2D} between the two DUEs is within a predefined range $[d_{min}, d_{max}]$ to guarantee the basic transmission quality. d_{min} is a very short distance representing the minimum physical separation between any two UEs, and d_{max} is jointly determined by the SIR threshold δ_D required for a DUE's successful reception and other network parameters.

Compared with the autonomous D2D communications, the CUE's transmission can always be coordinated by the BS. In view of the near-far effect, we assume that the average power of the CUE uplink transmission received at the BS is always controlled to the same level $P_{r,CB}$[10]. Therefore, the maximum CUE transmission power $P_{t,C_{max}}$ is utilized when the CUE is located on the boundary of the cell, hence $P_{r,CB} = \beta_B P_{t,C_{max}} / r^{\alpha_B}$. To eliminate the effect of the CUE's transmission on the D2D communications carried out with the same radio resource, all the DUE receivers should stay outside of the impact disk centered at the transmitting CUE with radius G_C as depicted in Fig. 1. Similarly, to guarantee the required SIR δ_B for successfully receiving a CUE's uplink transmission in one of the n_S sectors, there should be a minimum guard distance G_B between the BS and all the DUE transmitters in the sector, which limits the number of concurrent D2D pairs and the total interference accumulated at BS. With a similar method and model, the performance of the downlink reusing scenario could also be analyzed, which will be one of our research issues in the near future.

V. Derivation of Guard Distances

In this section, the guard distance G_D between two transmitting DUEs will be firstly determined based on the bound effect of the accumulated interference in large-scale wireless networks. After that, the maximum transmission range d_{max} for a D2D communication is derived with the help of the PED-based interference modeling method. By following the similar methods, guard distances G_C and G_B will also be calculated respectively. These four parameters will be used in the next section for obtaining the bound performance of D2D communications in a sector-partitioned cell.

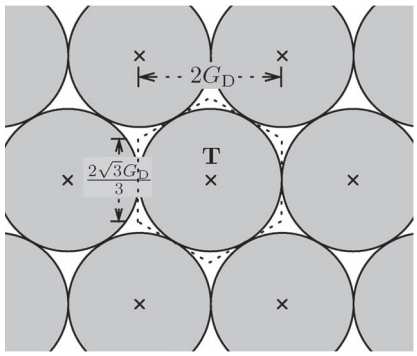

Fig. 2. Hexagon grid shaped by ERs of all the concurrent DUE transmitters.

A. Calculation of G_D

According to the results of circle/sphere packing in geometry [18], all the ERs of concurrent DUE transmitters will shape a hexagon grid with side length $\frac{2\sqrt{3}G_D}{3}$ as shown in Fig. 2, when they are arranged in the most compact way, which also represents the situation that the total signal power accumulated at network nodes reaches the maximum. By defining the most inner layer of the ERs surrounding the observation point (e.g., transmitter **T** shown in Fig. 2) as the 1-st layer, the interference power generated by all the l-layer transmitters (l is a natural number) can be calculated with the traditional discrete-style analysis method used in [1] as

$$I_{\mathbf{T}}(l) = 6I'_{\mathbf{T}}(l) - 6 \times \sum_{i=1}^{l} \frac{\beta_D P_{t,D}}{(2i\, G_D)^{\alpha_D}}, \tag{3}$$

where

$$I'_{\mathbf{T}}(l) = \sum_{i=1}^{l} \sum_{j=1}^{i+1} \frac{\beta_D P_{t,D}}{(d_{i,j}\, G_D)^{\alpha_D}}, \qquad \text{and} \tag{4}$$

$$d_{i,j} = \sqrt{4i^2 + 4(j-1)^2 - 4i(j-1)}. \tag{5}$$

On the other hand, due to the power attenuation, if a transmitter is located quite far away from the observation point **T**, its contribution to the accumulated signal power will be very small, or could even be ignored. Usually, this is regarded as the *bound effect* of the accumulated interference in large wireless networks [2], [19]. Moreover, for $\alpha_D > 2$, even with an infinity number of interferers, the total interference power is bounded and the aggregated interference from each layer decays [20]. Thus given a bounding level γ (e.g., 1% or 0.5%), which is depending on the expected analysis accuracy, the total signal

power received at **T** could be regarded as already bounded considering the first l layers, if

$$1-\frac{I_{\mathbf{T}}(l)-I_{\mathbf{T}}(l-1)}{I_{\mathbf{T}}(l-1)-I_{\mathbf{T}}(l-2)}\le\gamma. \tag{6}$$

By substituting (3) into (6), the minimum number of ER layers, $l_{\alpha_D,\gamma}$, for **T** to receive the bounded total signal power could be calculated by numerical methods when α_D and γ are known. Moreover, it is also clear that, when all the ERs are arranged in the densest way, the bounded reception power $I_{\mathbf{T}}(l_{\alpha,\gamma})$ can be approximated to the sensing threshold P_{th}, otherwise, the shaped ER grid just contradicts with the channel sensing process. Therefore, the guard distance G_D for a DUE transmitter could be derived from $P_{\text{th}}=I_{\mathbf{T}}(l_{\alpha_D,\gamma})$ as

$$G_D=\sqrt[\alpha_D]{\frac{6\beta_D P_{t,D}}{P_{\text{th}}}\left(\sum_{i=1}^{l_{\alpha_D,\gamma}}\sum_{j=1}^{i+1}\frac{1}{d_{i,j}^{\alpha_D}}-\sum_{i=1}^{l_{\alpha_D,\gamma}}\frac{1}{(2i)^{\alpha_D}}\right)}. \tag{7}$$

Considering that γ directly affects G_D's calculation, which might further influence the accuracy of the bound performance analysis, a group of simulation results will be shown in Section VII to demonstrate the impact of γ on the analysis error, and provide some guidelines for γ's value selection.

B. Calculation for $d_{\max}$

To guarantee a successful transmission between a DUE transmitter **T** and its DUE receiver **R**, the transmission distance d_{D2D} has to satisfy the SIR requirement δ_D as

$$\frac{\beta_D P_{t,D}/d_{D2D}^{\alpha_D}}{I_{\mathbf{R}}(d_{D2D})}\ge\delta_D, \tag{8}$$

where $I_{\mathbf{R}}(d_{D2D})$ is the interference accumulated at the observed receiver **R**. The calculation of $I_{\mathbf{R}}(d_{D2D})$ will become extremely complicated if following the discrete-style analysis used for obtaining G_D, as too many possible situations need to be analyzed individually. However, by utilizing the PED-based interference analysis method, the derivation process could be greatly simplified.

As briefly described in Section III, by building up a polar coordinates system shown in Fig. 3 with its origin located at the transmitter **T**, $I_{\mathbf{R}}(d_{D2D})$ can be calculated by an area integral as[3]

$$I_{\mathbf{R}}(d_{D2D})=\beta_D\lambda_{\alpha_D}\int_{\rho_1}^{\rho_2}\int_0^{2\pi}\frac{\rho\,d\rho\,d\theta}{D^{\alpha_D}}, \tag{9}$$

where

$$D=\sqrt{\rho^2+d_{D2D}^2+2\rho d_{D2D}\cos\theta}, \tag{10}$$

$\rho_1=G_D$, $\rho_2=(1+2l_{\alpha_D,\gamma})G_D$, and λ_{α_D} is the equivalent PED given the pathloss exponent α_D. Due to the complexity of the integral, the result of (9) could not be presented in a universal way for any value of α_D. But once α_D is known, $d_{\max}$ can always be determined as the maximum value of d_{D2D} to make

[3]For simplicity, only the part of concurrent transmitters contributing to the bounded interference accumulated at the observed receiver **R** are considered.

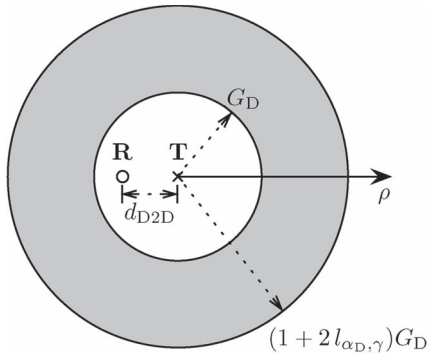

Fig. 3. PED-based calculation for the accumulated interference at receiver R (The ratio for the outer and inner radius of the shaded ring area is set for easy illustration and not to scale.).

(8) still hold. For example, if α_D is set to 4, which is the typical value for the D2D link in the cellular networks, the integral in (9) could be simplified as follow:

$$\begin{aligned}I_{\mathbf{R}}(d_{D2D})&=2\pi\beta_D\lambda_{\alpha_D}\int_{\rho_1}^{\rho_2}\frac{\rho\left(\rho^2+d_{D2D}^2\right)}{\left(d_{D2D}^2-\rho^2\right)^3}d\rho\\&=2\pi\beta_D\lambda_{\alpha_D}\left(\frac{(1+2l_{\alpha_D,\gamma})^2G_D^2}{2\left(d_{D2D}^2-(1+2l_{\alpha_D,\gamma})^2G_D^2\right)^2}-\frac{G_D^2}{2(d_{D2D}^2-G_D^2)^2}\right).\end{aligned} \tag{11}$$

By substituting (11) into (8), the only variable left is d_{D2D}, so $d_{\max}$ could be obtained easily by some search algorithms, e.g., the binary search algorithm.

C. Calculation for G_C

Based on the system model, no matter how many D2D pairs are active simultaneously, the impact of a transmitting CUE on each communicating DUE pair is independent with each other. Suppose a CUE node is located with distance d_{CB} to its BS, then its transmission power $P_{t,C}$ can be represented as

$$P_{t,C}=\frac{P_{r,CB}\,d_{CB}^{\alpha_B}}{\beta_B}=P_{t,C_{\max}}\cdot\left(\frac{d_{CB}}{r}\right)^{\alpha_B}. \tag{12}$$

Similarly, considering the SIR constraint at DUE, we have

$$\delta_D\le\frac{\beta_D P_{t,D}/d_{D2D}^{\alpha_D}}{\beta_D P_{t,C}/d_{CD}^{\alpha_D}}=\frac{P_{t,D}}{P_{t,C}}\left(\frac{r}{d_{CB}}\right)^{\alpha_B}\left(\frac{d_{CD}}{d_{D2D}}\right)^{\alpha_D}, \tag{13}$$

where d_{CD} is the distance between the CUE and the interfered DUE node. To determine G_C for system setting, the worst case for a being affected D2D pair, which has the longest transmission distance ($d_{D2D}=d_{\max}$), should be considered. Therefore, G_C can be obtained as a function of d_{CB} as

$$G_C=K\cdot\sqrt[\alpha_D]{d_{CB}^{\alpha_B}}, \tag{14}$$

where

$$K=d_{\max}\cdot\sqrt[\alpha_D]{\frac{\delta_D P_{t,C_{\max}}}{r^{\alpha_B}P_{t,D}}}. \tag{15}$$

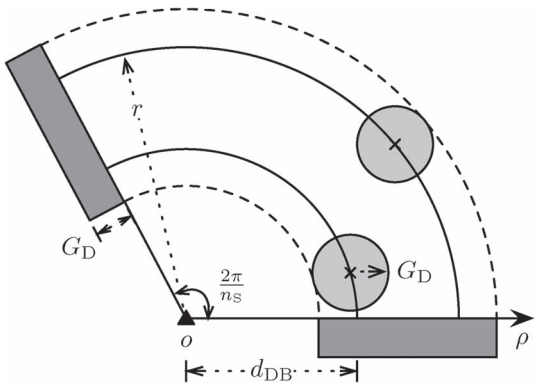

Fig. 4. Calculation of G_B, given n_S.

Theoretically, K could be changed from 0 to a very large number, but based on the reasonable parameter settings of the cellular system, K should be always larger than 1. Therefore, the BS is always covered by the CUE's impact disk, and this condition will be utilized in the following analysis.

D. Calculation for G_B

For one of the n_S sectors, given that the distance between any active DUE transmitter and the BS is no shorter than d_{DB} as shown in Fig. 4, the accumulated interference power received at the BS $I_B(n_S)$ reaches its maximum when the CUE's impact disk is fully included inside the BS's guard region, which means that the number of concurrent D2D pairs in the observed sector area reaches the maximum. By following the PED-based method, $I_B(n_S)$ could be calculated as

$$I_B(n_S) = \beta_B \lambda_{\alpha_B} \left(\int_0^{\frac{2\pi}{n_S}} \int_{d_{DB}-G_D}^{r+G_D} \frac{\rho d\theta d\rho}{\rho^{\alpha_D}} + \Theta \right), \tag{16}$$

where Θ is the part of the interference equivalently generated from the two shaded rectangular area in Fig. 4. Θ's expression could be given as

$$\begin{aligned}\Theta =& 2\beta_B \lambda_{\alpha_B} \left(\int_0^{\theta_1} \int_{d_{DB}/\cos\theta}^{r/\cos\theta} \frac{\rho d\rho d\theta}{\rho^{\alpha_B}} + \int_{\theta_1}^{\theta_2} \int_{d_{DB}/\cos\theta}^{G_D/\sin\theta} \frac{\rho d\rho d\theta}{\rho^{\alpha_B}} \right) \\ =& \frac{2\beta_B \lambda_{\alpha_B}}{\alpha - 2} \left(\frac{\int_0^{\theta_2} (\cos\theta)^{\alpha_B - 2} d\theta}{d_{DB}^{\alpha_B - 2}} - \frac{\int_0^{\theta_1} (\cos\theta)^{\alpha_B - 2} d\theta}{r^{\alpha_B - 2}} \right. \\ & \left. - \frac{\int_{\theta_1}^{\theta_2} (\sin\theta)^{\alpha_B - 2} d\theta}{d_{\max}^{\alpha_B - 2}} \right),\end{aligned} \tag{17}$$

where $\theta_1 = \arctan\frac{G_D}{r}$ and $\theta_2 = \arctan\frac{G_D}{d_{DB}}$. The final integral result of (17) is related to the hypergeometric function [21], which is not easy to be utilized for deriving G_B with (16) and δ_B. On the other hand, considering the actual ratio of G_D and r for the D2D communication scenario, the impact of Θ on the total interference accumulated at BS is relatively small. Therefore, we ignore Θ in (16) as

$$\begin{aligned}I_B(n_S) \approx& \beta_B \lambda_{\alpha_B} \int_0^{\frac{2\pi}{n_S}} \int_{d_{BD}-G_D}^{r+G_D} \frac{\rho d\theta d\rho}{\rho^{\alpha_B}} \\ =& \frac{2\pi\beta_B \lambda_{\alpha_B} \left((d_{DB} - G_D)^{2-\alpha_B} - (r+G_D)^{2-\alpha_B} \right)}{n_S(\alpha_B - 2)}.\end{aligned} \tag{18}$$

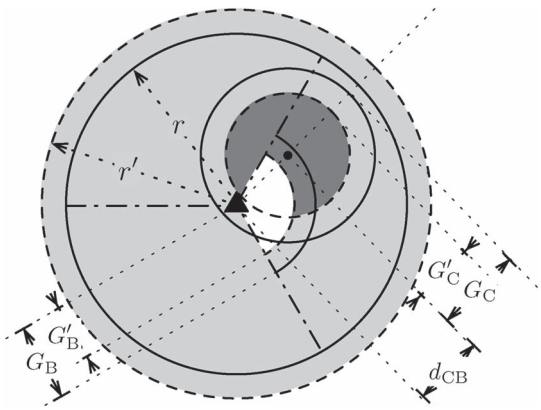

Fig. 5. Network area left for D2D communications utilizing identical uplink resources, when $n_S = 3$.

The approximation error of (18) is zero when $n_S = 1$, and more accurate analysis of $I_B(n_S)$ for $n_S > 1$ is one of our further research issues. Considering the SIR requirement δ_B at BS, a ratio relation has to be held as

$$\delta_B \le \frac{P_{r,CB}}{I_B(n_S)} = \frac{\beta_B P_{t,C_{max}}}{r^{\alpha_B} I_B(n_S)}, \tag{19}$$

and finally, G_B could be determined by

$$G_B = G_D + \sqrt[2-\alpha_B]{\frac{n_S(\alpha_B - 2)P_{t,C_{max}}}{2\pi\delta_B \lambda_{\alpha_B} r^{\alpha_B}} + (r+G_D)^{2-\alpha_B}}. \tag{20}$$

VI. Analysis of Bound Performance

For the n_S sectors in the observed cell, there are different ways to allocate the available uplink radio resources, which may further affect the total performance gain provided by D2D communications. To describe all the possible cases, it is assumed that the overall radio resources of the cell can be evenly divided into n_f parts ($n_S \ge n_f$), and n_f should be a factor number of n_S (for example, if $n_S = 6$, n_f should be either 1, 2, 3, or 6). In this section, we will start from analyzing the special case when $n_S = n_f$, which means that the orthogonal resource blocks with identical bandwidth W/n_S are allocated to each sector respectively, and W is the total bandwidth. Although this might be counterintuitive, especially when the directional antennas are deployed for sector partition, the bound performance of this specific case is relatively easy to be obtained, and can be further extended to other more realistic resource allocation cases smoothly.

A. Orthogonal Frequency Allocation Case

Different from the extreme situation for obtaining G_B, the CUE's impact disk could be moved out of the BS's guard region in a more general scenario, so the total area left for deploying D2D communications is reduced. Owing to the directional antenna and the orthogonal resource allocation scheme, for a specific sector and given d_{CB}, the whole network area left for deploying the D2D ERs reusing the sector's uplink resource is illustrated in Fig. 5 as the light shaded region. According

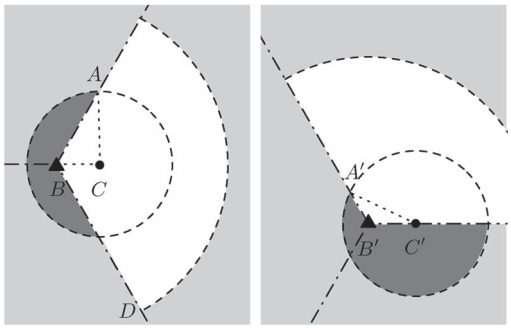

Fig. 6. Illustration of $\mathcal{S}_{\text{o,min}}$ and $\mathcal{S}_{\text{o,max}}$, when the CUE's impact disk is inside BS's guard region.

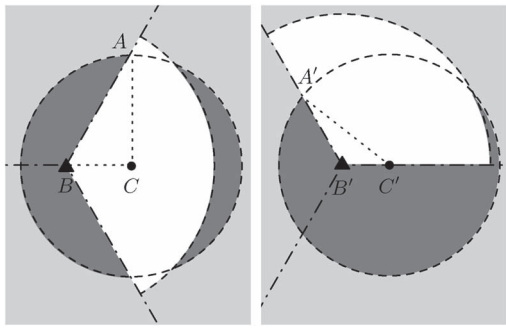

Fig. 7. Illustration of $\mathcal{S}_{\text{o,min}}$ and $\mathcal{S}_{\text{o,max}}$, when the CUE's impact disk partially moves out of BS's guard region, but is still fully included in the cell area.

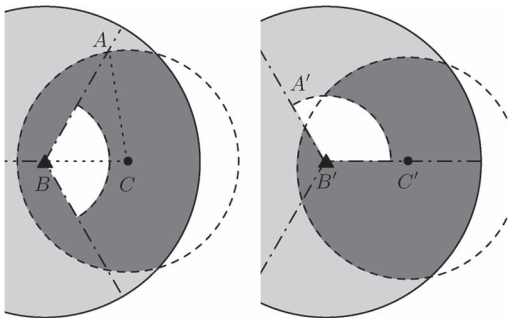

Fig. 8. Illustration of $\mathcal{S}_{\text{o,min}}$ and $\mathcal{S}_{\text{o,max}}$, when the CUE's impact disk partially moves out of the cell's coverage area.

to the system model, the DUE transmitter could be located on the boundary of the cell, the CUE's impact disk, and the BS's guard region, so the area of the light shaded region should be calculated as

$$\mathcal{S}(d_{\text{CB}}, n_{\text{S}}) = \pi r'^2 - \frac{1}{n_{\text{S}}}\pi G_{\text{B}}'^2 - \mathcal{S}_{\text{o}}, \tag{21}$$

where $r' = r + G_{\text{D}}$, $G'_{\text{B}} = G_{\text{B}} - G_{\text{D}}$, and $\mathcal{S}_{\text{o}}$ is the network area occupied by the CUE's impact disk (the dark shaded part in Fig. 5). In view of the numerous possible relative positions of BS and CUE, fully exploring $\mathcal{S}_{\text{o}}$'s expression will be prohibitively complicated. However, when d_{CB} is given, $\mathcal{S}_{\text{o}}$ reaches its minimum when the CUE is located on the midline of the observed sector, and goes to the maximum when the CUE is on the sector's radii.[4] Therefore, $\mathcal{S}_{\text{o}}$'s extreme situations can always be derived and contribute to the throughput improvement's bound analysis. Furthermore, to distinguish the overlap situations between the CUE's impact disk, BS's guard region, and the cell area, $d_{\text{CB}} \in (0, r_{\text{C}}]$ can be divided into three different intervals as follows.

When $d_{\text{CB}} \in [0, d_{\text{th1}})$, where d_{th1} can be derived by $G'_{\text{B}} = d_{\text{th1}} + G'_{\text{C}} (G'_{\text{C}} = G_{\text{C}} - G_{\text{D}})$, the CUE's impact disk is always fully inside the BS's guard region. In this case, the two extreme situations of $\mathcal{S}_{\text{o}}$ are illustrated in Fig. 6, and can be calculated respectively as

$$\mathcal{S}^{\mathbf{1}}_{\text{o,min}} = \angle BCA \cdot \overline{AC}^2 - \overline{BC} \cdot \overline{AB} \cdot \sin\angle ABC, \tag{22}$$

$$\mathcal{S}^{\mathbf{1}}_{\text{o,max}} = \frac{(\angle B'C'A' + \pi)\overline{A'C'}^2}{2} - \frac{\overline{B'C'} \cdot \overline{A'B'} \cdot \sin\angle A'B'C'}{2}, \tag{23}$$

where $\angle ABC = \pi / n_{\text{S}}$, $\angle A'B'C' = 2\pi / n_{\text{S}}$, $\overline{BC} = \overline{B'C'} = d_{\text{CB}}$, $\overline{AC} = \overline{A'C'} = G'_{\text{C}}$. According to the Law of Cosine, $\overline{AB}$, $\angle BCA$, $\overline{A'B'}$, and $\angle B'C'A'$ could be also calculated, but their expressions are omitted here. The superscript **1** is used to identify the d_{CB}'s first possible interval.

When $d_{\text{CB}} \in [d_{\text{th1}}, d_{\text{th2}})$, where d_{th2} could be derived by $r' = d_{\text{th2}} + G'_{\text{C}}$, the CUE's impact disk partially crosses the BS's guard region's boundary but is still fully included within the cell area. For this case, the two extreme situations of $\mathcal{S}_{\text{o}}$ are illustrated in Fig. 7, and could be presented respectively as

$$\mathcal{S}^{\mathbf{2}}_{\text{o,min}} = \mathcal{S}^{\mathbf{1}}_{\text{o,min}} + \pi G_{\text{C}}'^2 - \mathcal{F}\left(G'_{\text{B}}, G'_{\text{C}}, d_{\text{CB}}\right), \tag{24}$$

$$\mathcal{S}^{\mathbf{2}}_{\text{o,max}} = \mathcal{S}^{\mathbf{1}}_{\text{o,max}} + \frac{1}{2}\left(\pi G_{\text{C}}'^2 - \mathcal{F}\left(G'_{\text{B}}, G'_{\text{C}}, d_{\text{CB}}\right)\right), \tag{25}$$

where $\mathcal{F}(x, y, z)$ represents the overlapping area of two disks with radius x and y, which are located with center distance z away from each other. The detailed expression of $\mathcal{F}(x, y, z)$ could be found in the Appendix of [1].

Finally, when $d_{\text{CB}} \in [d_{\text{th2}}, r_{\text{C}}]$, the CUE's impact disk partially moves out of the cell's coverage area, and the two extreme situations of $\mathcal{S}_{\text{o}}$ are illustrated in Fig. 8. With the similar method, $\mathcal{S}_{\text{o,min}}$ and $\mathcal{S}_{\text{o,max}}$ for this case could be calculated as

$$\mathcal{S}^{\mathbf{3}}_{\text{o,min}} = \mathcal{F}\left(r', G'_{\text{C}}, d_{\text{CB}}\right) - \frac{1}{n_{\text{S}}}\pi G_{\text{C}}'^2, \tag{26}$$

$$\mathcal{S}^{\mathbf{3}}_{\text{o,max}} = \mathcal{S}^{\mathbf{1}}_{\text{o,max}} - \frac{1}{2}\pi G_{\text{C}}'^2 + \mathcal{F}\left(r', G'_{\text{C}}, d_{\text{CB}}\right) - \frac{1}{2}\mathcal{F}\left(G'_{\text{B}}, G'_{\text{C}}, d_{\text{CB}}\right). \tag{27}$$

With the above analytical results of $\mathcal{S}(d_{\text{CB}}, n_{\text{S}})$[5], and considering that each ER actually occupies a hexagonal network area with side length $\frac{2\sqrt{3}G_{\text{D}}}{3}$ in the densest arrangement situation as mentioned in Section V-A, the upper and lower bound for

[4]Due to the space limit, the detailed proof and verification of the conditions for $\mathcal{S}_{\text{o}}$ to reach its maximum and minimum are not included in this paper, but can be found at http://grp.pan.uvic.ca/~mmni/pubs/area_proof.pdf.

[5]To improve the reproducibility of $\mathcal{S}(d_{\text{CB}}, n_{\text{S}})$ related analysis, the Matlab code for the piecewise function $\mathcal{S}(d_{\text{CB}}, n_{\text{S}})$, which has integrated (21)–(27) completely, is available for download from http://grp.pan.uvic.ca/~mmni/pubs/Func_S.m.

the maximum number of D2D pairs reusing identical uplink resources in the observed cell can be approximated by

$$n_{\mathrm{U}}(d_{\mathrm{CB}},n_{\mathrm{S}}) \approx \frac{\mathcal{S}(d_{\mathrm{CB}},n_{\mathrm{S}})|_{\mathcal{S}_{\mathrm{o}}=\mathcal{S}^{\mathbf{x}}_{\mathrm{o,min}}}}{2\sqrt{3}G_{\mathrm{D}}^2}, \tag{28}$$

$$n_{\mathrm{L}}(d_{\mathrm{CB}},n_{\mathrm{S}}) \approx \frac{\mathcal{S}(d_{\mathrm{CB}},n_{\mathrm{S}})|_{\mathcal{S}_{\mathrm{o}}=\mathcal{S}^{\mathbf{x}}_{\mathrm{o,max}}}}{2\sqrt{3}G_{\mathrm{D}}^2}, \tag{29}$$

where $\mathbf{x}$ could be either 1, 2, or 3, depending on d_{CB}'s actual value. It is clear that, the total throughput improvement $\mathcal{T}(d_{\mathrm{CB}},n_{\mathrm{S}})$ of the entire cell reaches it upper bound when all the concurrent D2D pairs are communicating with the closest transmission range as

$$\mathcal{T}_{\mathrm{U}}(d_{\mathrm{CB}},n_{\mathrm{S}}) = n_{\mathrm{S}}\cdot n_{\mathrm{U}}(d_{\mathrm{CB}},n_{\mathrm{S}})\cdot \frac{R_b(d_{\mathrm{D2D}})}{n_{\mathrm{S}}}\bigg|_{d_{\mathrm{D2D}}=d_{\min}}, \tag{30}$$

where $R_b(d_{\mathrm{D2D}})$ is the capacity of a D2D link with transmission distance d_{D2D} when the bandwidth is W, which could be calculated according to the Shannon theorem

$$R_b(d_{\mathrm{D2D}}) = W\log_2\left(1+\frac{\beta_{\mathrm{D}}\,P_{\mathrm{t,D}}}{d_{\mathrm{D2D}}^{\alpha_{\mathrm{D}}}\,I_{\mathbf{R}}(d_{\mathrm{D2D}})}\right). \tag{31}$$

Similarly, $\mathcal{T}(d_{\mathrm{CB}},n_{\mathrm{S}})$ goes to its lower bound when all the concurrent D2D pairs are communicating with distance $d_{\max}$ as

$$\mathcal{T}_{\mathrm{L}}(d_{\mathrm{CB}},n_{\mathrm{S}}) = n_{\mathrm{L}}(d_{\mathrm{CB}},n_{\mathrm{S}})\cdot R_b(d_{\max}). \tag{32}$$

If we further assume that all the UEs are uniformly distributed in the cell, when d_{CB} is given, the expectation of the CUE's position should be on the midline of the sector, which leads to $n_{\mathrm{U}}(d_{\mathrm{CB}},n_{\mathrm{S}})$. Therefore, the expectation of the maximum throughput improvement could be calculated as

$$\overline{\mathcal{T}(d_{\mathrm{CB}},n_{\mathrm{S}})} = n_{\mathrm{U}}(d_{\mathrm{CB}},n_{\mathrm{S}})\cdot R_b(\overline{d_{\mathrm{D2D}}}), \tag{33}$$

where

$$\overline{d_{\mathrm{D2D}}} = \frac{2\left(d_{\max}^3-d_{\min}^3\right)}{3\left(d_{\max}^2-d_{\min}^2\right)}. \tag{34}$$

B. General Frequency Allocation Cases

For more intuitive description, Fig. 9 is used to demonstrate the impact of different frequency allocation cases on the area left for deploying D2D communications, when n_{S} is set to 6. The different gray levels in each allocation scheme are used to represent the different resource blocks, which is determined by n_{f}.

When $n_{\mathrm{f}}=1$, the whole resource block is reused in each sector, which is shown in Fig. 9(a). If we ignore the CUE's impact on D2D communications in each sector, the maximum throughput improvement could be calculated with the similar method used in the previous section as

$$\mathcal{T}'(n_{\mathrm{f}}=1) = n_{\mathrm{S}}\cdot\frac{\mathcal{S}_{\mathrm{R}}}{2\sqrt{3}G_{\mathrm{D}}^2\,n_{\mathrm{S}}}\cdot R_b(d_{\mathrm{D2D}}) = \mathcal{S}_{\mathrm{R}}\cdot\frac{R_b(d_{\mathrm{D2D}})}{2\sqrt{3}G_{\mathrm{D}}^2}, \tag{35}$$

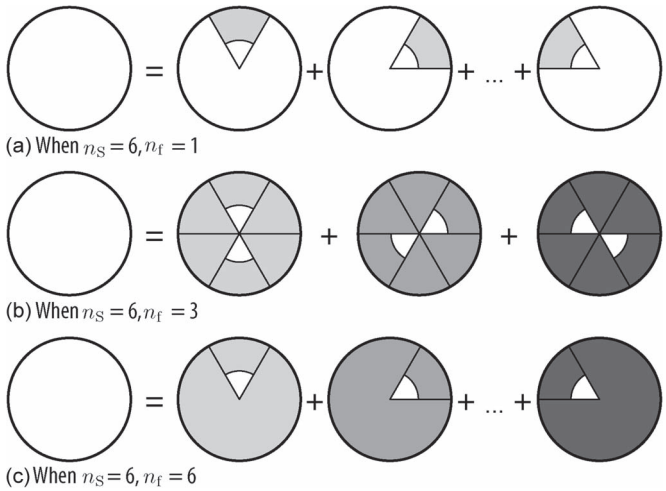

Fig. 9. An illustration of different resource allocation schemes for D2D communications in each sector, given $n_{\mathrm{S}}=6$.

where $\mathcal{S}_{\mathrm{R}}$ is the area of the ring region with inner radius G'_{B} and outer radius r', and $R_b(d_{\mathrm{D2D}})$ has already been given in (31). Comparing with the non-sectorized situation, the interference power received at the BS is greatly reduced due to the feature of directional antennas. Therefore, the ring area $\mathcal{S}_{\mathrm{R}}$ is also increased significantly, which will lead to an obvious improvement of the network throughput provided by the D2D communications.

When $1<n_{\mathrm{f}}<n_{\mathrm{S}}$, the whole resource block is divided into n_{f} parts, each with bandwidth W/n_{f}. For one of the n_{f} resource blocks, it is designated for $n_{\mathrm{S}}/n_{\mathrm{f}}$ sectors' cellular uplink transmission, moreover, it could also be reused in all the other $n_{\mathrm{S}}-n_{\mathrm{S}}/n_{\mathrm{f}}$ sectors for D2D communications. As shown in Fig. 9(b), when $n_{\mathrm{S}}=6$, $n_{\mathrm{f}}=2$, each resource block can be used for D2D communications within one third of the entire ring area $\mathcal{S}_R$ and also two thirds of the whole cell. Similarly, without the CUE's impact, the maximum throughput improvement can be calculated as

$$\begin{aligned}\mathcal{T}'(1<n_{\mathrm{f}}<n_{\mathrm{S}}) &= n_{\mathrm{f}}\cdot\frac{\frac{\mathcal{S}_{\mathrm{R}}}{n_{\mathrm{f}}}+\left(1-\frac{1}{n_{\mathrm{f}}}\right)\frac{\mathcal{S}_{\mathrm{D}}}{n_{\mathrm{S}}}}{2\sqrt{3}G_{\mathrm{D}}^2}\cdot\frac{R_b(d_{\mathrm{D2D}})}{n_{\mathrm{f}}}\\ &= \left(\frac{\mathcal{S}_{\mathrm{R}}}{n_{\mathrm{f}}}+\frac{(n_{\mathrm{f}}-1)\mathcal{S}_{\mathrm{D}}}{n_{\mathrm{f}}\,n_{\mathrm{S}}}\right)\cdot\frac{R_b(d_{\mathrm{D2D}})}{2\sqrt{3}G_{\mathrm{D}}^2},\end{aligned} \tag{36}$$

where $\mathcal{S}_{\mathrm{D}}$ is the area of the disk with radius r'.

When $n_{\mathrm{f}}=n_{\mathrm{S}}$, it is identical to the orthogonal resource allocation scheme discussed earlier and shown in Fig. 9(c). By ignoring the CUE's impact, the maximum throughput improvement can be calculated as

$$\begin{aligned}\mathcal{T}'(n_{\mathrm{f}}=n_{\mathrm{S}}) &= n_{\mathrm{f}}\cdot\frac{\frac{\mathcal{S}_{\mathrm{R}}}{n_{\mathrm{S}}}+\frac{n_{\mathrm{S}}-1}{n_{\mathrm{S}}}\mathcal{S}_{\mathrm{D}}}{2\sqrt{3}G_{\mathrm{D}}^2}\cdot\frac{R_b(d_{\mathrm{D2D}})}{n_{\mathrm{f}}}\\ &= \left(\frac{\mathcal{S}_{\mathrm{R}}}{n_{\mathrm{S}}}+\frac{(n_{\mathrm{S}}-1)\mathcal{S}_{\mathrm{D}}}{n_{\mathrm{S}}}\right)\cdot\frac{R_b(d_{\mathrm{D2D}})}{2\sqrt{3}G_{\mathrm{D}}^2}.\end{aligned} \tag{37}$$

Based on the condition $1\le n_{\mathrm{f}}\le n_{\mathrm{S}}$, it is clear that

$$S_{\mathrm{R}} < \frac{\mathcal{S}_{\mathrm{R}}}{n_{\mathrm{f}}}+\frac{(n_{\mathrm{f}}-1)\mathcal{S}_{\mathrm{D}}}{n_{\mathrm{f}}n_{\mathrm{S}}} < \frac{\mathcal{S}_{\mathrm{R}}}{n_{\mathrm{S}}}+\frac{(n_{\mathrm{S}}-1)\mathcal{S}_{\mathrm{D}}}{n_{\mathrm{S}}}. \tag{38}$$

which means that, in the extreme situations when the CUE's impact is not considered, more complicated resource allocation scheme (larger n_f) also leads to a higher throughput improvement. This pattern will be kept when the CUE's impact is also considered. However, considering that the varying is only caused by the difference between $\mathcal{S}_R$ and $\mathcal{S}_D$, it will not be obvious when G_B is relatively small, which is common in the D2D communications-enabled cellular systems. Therefore, when the system complexity is concerned, we could use simple resource allocation schemes to achieve a similar performance improvement for the D2D communications.

VII. Performance Evaluation

In this section, the analytical results obtained in the previous sections will be validated by Monte Carlo simulations, which are all finished in Matlab. All the UEs in the observed cell are uniformly distributed with high density. The common parameters for the simulations are set as: bounding level $\gamma = 0.01$, sensing threshold $P_{th} = 0.005$ mW, the minimum physical separation between two UEs $d_{min} = 2$ m, system bandwidth $W = 5$ MHz, and SIR thresholds $\delta_B = 10$ dB and $\delta_D = 13$ dB. By referring to [22], the path-loss with the propagation distance d (m) is set to $L(d)(\text{dB}) = 15.3 + 37.6\log_{10}(d)$ for the CUE-BS link, and $L(d)(\text{dB}) = 28 + 40\log_{10}(d)$ for the D2D transmission, respectively.

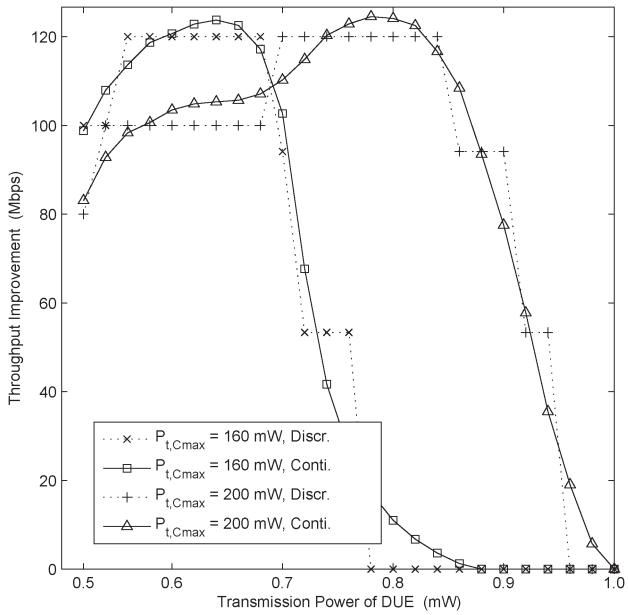

Fig. 10. Continuous- and discrete-style analysis results for throughput improvement ($n_S = 1$) vs. $P_{t,D}$ ($d_{CB} \to 0$, $r = 500$ m, $R_b = 2$ Mbps).

A. Comparison Between the Discrete and Continuous Analysis

The analytical results derived with the continuous-style analysis in this paper are first compared with the ones obtained by the discrete-style method in [1]. Considering the validity of the comparison, all the parameter settings and assumptions are set identical to our previous work as much as possible. Moreover, the variable transmission bit-rate model applied in this paper, which is determined by the actual SIR, is also simplified to the constant bit-rate model used in [1], and n_S is set to 1 for this simulation group.

In Fig. 10, the results of the throughput improvement provided by D2D communications, when the CUE's impact disk is fully included inside the BS's guard region, are presented with changing DUE transmission power $P_{t,D}$ and maximum CUE transmission power $P_{t,C_{max}}$, for both the discrete- and continuous-style analysis. It is intuitive that, increasing $P_{t,D}$ can support the same bit-rate with a relatively shorter guard distance G_D, but the accumulated interference at the BS from all the concurrent D2D pairs will be greatly increased. Finally, the BS will need a longer guard distance G_B to guarantee the quality of CUE's uplink transmission, which reduces the total number of coexisting D2D pairs in the observed cell area. Therefore, once the system settings are fixed, there should be an optimal value or range of $P_{t,D}$ to achieve the optimal throughput improvement. This prediction is verified in Fig. 10, and it shows that the optimal value of $P_{t,D}$ is increased with $P_{t,C_{max}}$. Moreover, the changing pattern demonstrated in the continuous-style analysis's results matches the staged increasing and decreasing characteristic of the discrete analysis results. Similarly, when the CUE is outside the BS's guard region, the results obtained from the continuous- and discrete-style analysis also match with each other as well. Due to the space limit, the comparison is omitted here.

B. Comparison Between the Simulation and Analytical Results

In this simulation group, all the assumptions used in the previous group for matching the discrete-style analysis carried out in our earlier work are removed. While still keeping both the simulation and analytical results in different figures easy to be compared with each other, relatively large variation ranges are set for the variables in this group as: $P_{t,D} = 0.5 \sim 0.9$ mW, $P_{t,C_{max}} = 50 \sim 150$ mW, and $r = 300 \sim 800$ m.

For the situation that the entire cell is a single sector ($n_S = 1$), the simulation and analytical results for the expectation of the maximum throughput improvement $\overline{\mathcal{T}(d_{CB}, 1)}$ are illustrated in Fig. 11, when the cell radius r is fixed at 500 meters. As shown in the figure, the throughput improvement is independent of d_{CB} at the very beginning, which represents the scenario that the CUE's impact disk is fully included in the BS's guard region. When $d_{CB} > d_{th1}$, which means that the CUE's impact disk starts to partially intersect with the ring area determined by r and G_B, the number of D2D pairs shrinks, and so does the maximum throughput improvement. Moreover, the impact of the bounding level γ on analysis accuracy is also demonstrated in Fig. 11. It is clear that, when γ is set to a relative small value (e.g., 0.01), the difference between the theoretical and simulation results is small or can even be ignored. However, when the bounding level is relaxed to a larger value, the analytical error is also increased. This is because that, larger γ can be achieved by fewer layers of surrounding ERs, which means the interference power used for the analysis will be lower than the actual value. Therefore, with the increase of γ, the analytical error between the theoretical and simulation results are also gradually increased. Accordingly, when the

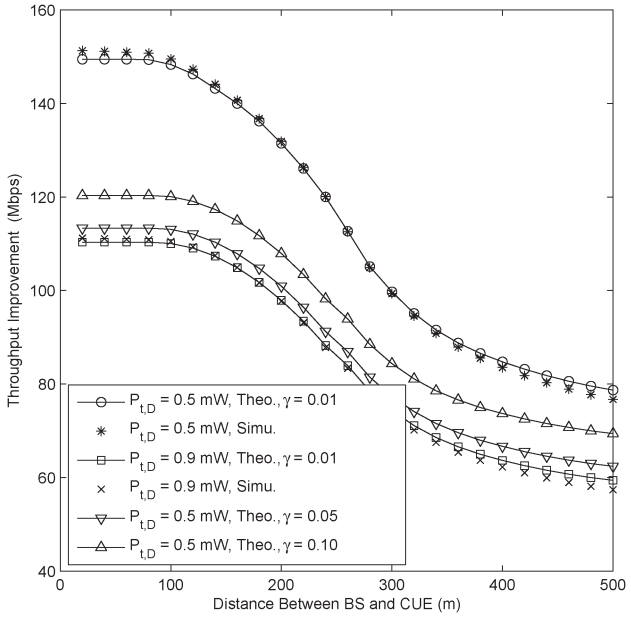

Fig. 11. $\overline{\mathcal{T}(d_{\mathrm{CB}},1)}$ vs. d_{CB} ($P_{\mathrm{t,C_{max}}} = 150$ mW, $r = 500$ m).

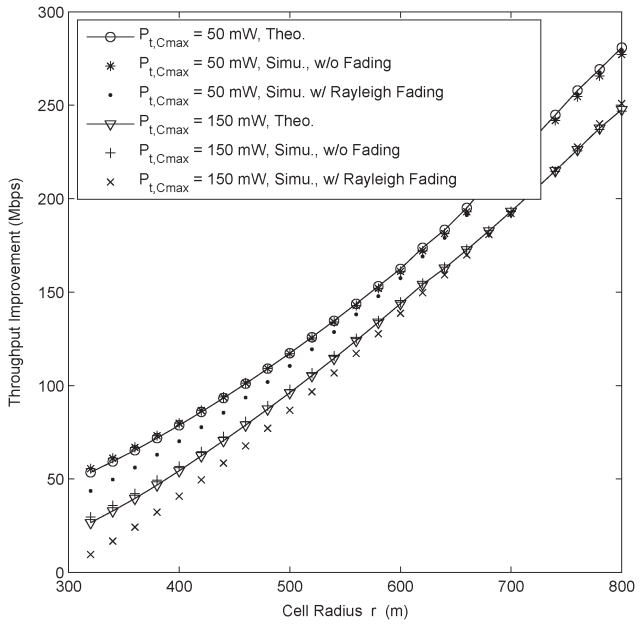

Fig. 12. $\overline{\mathcal{T}(d_{\mathrm{CB}},1)}$ vs. r ($d_{\mathrm{CB}} = \frac{2}{3}r$, $P_{\mathrm{t,D}} = 0.7$ mW).

computation complexity of the minimum bounding layer $l_{\alpha_{\mathrm{D}},\gamma}$ is still acceptable, the value of γ should be as small as possible for a better analysis accuracy.

When the cell radius r is relaxed to a variable, and d_{CB} is fixed at its expectation, which is $\frac{2}{3}r$ since all the UEs are assumed to be uniformly distributed, the simulation and analytical results of the average throughput improvement $\overline{\mathcal{T}(d_{\mathrm{CB}},1)}$ are illustrated in Fig. 12. It is clear that the matching degree between the simulation and theoretical analysis is still good, and the throughput improvement is monotonously increasing with the cell radius r. Although a larger r indicates a longer d_{CB} in the simulation, which further leads to a longer guard distance G_{C}, the increased CUE impact disk area will always

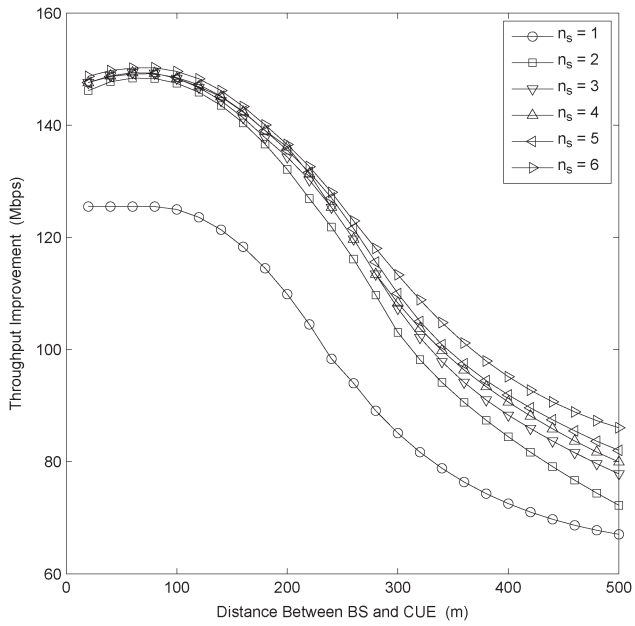

Fig. 13. $\overline{\mathcal{T}(d_{\mathrm{CB}},n_{\mathrm{S}})}$ vs. d_{CB} ($P_{\mathrm{t,C_{max}}} = 150$ mW, $P_{\mathrm{t,D}} = 0.7$ mW, $r = 500$ m).

be smaller than the increment of the entire cell area, so the total throughput improvement will keep increasing. But considering the constraint of CUE's maximum transmission power in the realistic scenario, r also has to be limited within a reasonable dynamic range. On the other hand, the simulation results when the Rayleigh fading is considered are also included in Fig. 12 for comparison. It is clear that, although the changing pattern still remains the same, the channel fading does deteriorate the throughput performance, and the gap between the cases with/without fading becomes more obvious with the increased transmission power or decreased cell radius. This is mainly due to the fact that, the Rayleigh fading makes the received signal power follow the exponential distribution, whose variance is directly determined by the distance-determined pathloss component. We have made some efforts to incorporate the channel fading into the PED-based modeling method for obtaining more general results. Some of our ideas and progresses for this topic are summarized as a brief discussion in Section VIII.

For the situation when the sector partition is enabled ($n_{\mathrm{S}} > 1$), the analytical results of $\overline{\mathcal{T}(d_{\mathrm{CB}},n_{\mathrm{S}})}$ are illustrated in Fig. 13. Although it is more meaningful to set n_{S} to some specific values such as 3 and 6 due to the frequency reuse patterns utilized in the real cellular system, n_{S} is changed from 2 to 6 in Fig. 13 for demonstrating a general performance changing pattern. Besides, the performance bounds and expectations for $n_{\mathrm{S}} = 1$ and $n_{\mathrm{S}} = 3$ are summarized together in Fig. 14. The first difference observed between the results of $n_{\mathrm{S}} = 1$ and $n_{\mathrm{S}} > 1$ is that, when $d_{\mathrm{CB}} < d_{\mathrm{th1}}$, $\overline{\mathcal{T}(d_{\mathrm{CB}},n_{\mathrm{S}})}$ is no longer a constant determined by G_{B}. This is because that, although the CUE's impact disk does not cross the boundary of the sector's BS guard region, it still occupies part of the network area in other sectors as shown in Figs. 6–8. Moreover, according to Fig. 13, it is clear that, the throughput improvement is obvious for all the possible d_{CB}, when n_{S} is changed from 1 to 2. But when n_{S} is further changed from 2 to larger values, the throughput improvement will only be apparent when d_{CB} is relatively large.

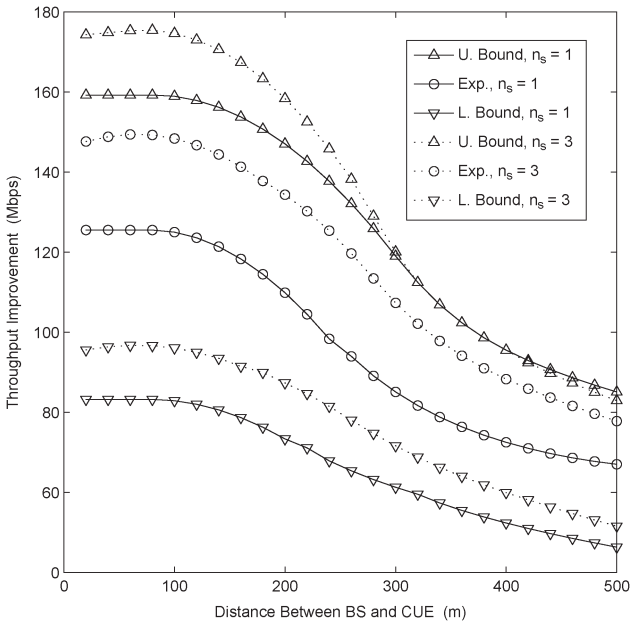

Fig. 14. Throughput bounds with identical parameter sets but different n_S ($P_{t,C_{max}} = 15$ mW, $P_{t,D} = 0.7$ mW, $r = 500$ m).

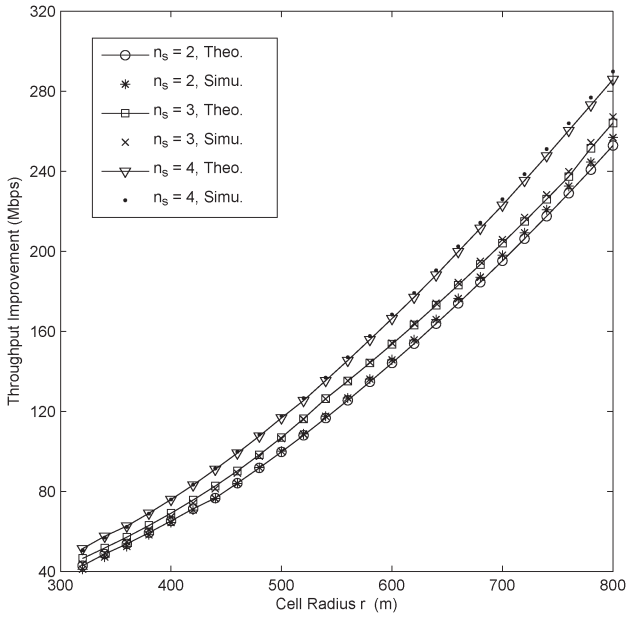

Fig. 15. $\overline{\mathcal{T}(d_{CB}, n_S)}$ vs. r ($d_{CB} = \frac{2}{3}r$, $P_{t,D} = 0.7$ mW, $P_{t,C_{max}} = 150$ mW).

These interesting phenomena are mainly due to the impact of changed n_S on G_B. With the orthogonal resource allocation scheme described in Section VI-A, a larger n_S directly reduces the accumulated interference, which leads to a shorter G_B. This variation causes the most obvious performance change when n_S is changed from 1 to 2, but its effect will decrease when n_S is further increased. In general, a larger n_S can provide a better throughput improvement of D2D communications, when the uplink resource of the whole cell is orthogonally allocated to each sector. But considering the increased complexity with a larger n_S, the sector number should be chosen based on the trade-off between the system performance and cost.

Similar to the settings used for Fig. 12, the simulation and analytical results of $\overline{\mathcal{T}(d_{CB}, n_S)}$ with different n_S, when $d_{CB} = \frac{2}{3}r$, are shown in Fig. 15. Comparing with the results when $n_S = 1$, increased sector number results in a larger throughput improvement with the same reason described earlier.

VIII. Further Discussion

Although we have validated the effectiveness and accuracy of the PED-based interference modeling method and the derived bound performance of D2D communications in a sector-partitioned cell, there still exists quite a lot of interesting and important follow-on work to be finished for further evolving the new analysis method itself. In this section, we will briefly discuss the major difficulties and our recent progress on: 1) applying the PED-based method for the sparse network scenarios; and 2) introducing the effect of channel fading into the PED-based modeling method.

According to the descriptions and applications of the PED-based method in the previous sections, it is clear that, the newly proposed continuous-style analysis is quite useful for obtaining the network bound performance, when all the coexisted ERs create a hexagon grid representing the worst-interfered case for all the network nodes. However, when the network density or traffic intensity is relatively low, the sum of all the concurrent ERs will become much smaller than the entire network region, which means the condition for carrying out the area integral presented in (2) may no longer be satisfied. In other words, the PED-based analysis method cannot be utlized for the sparse network in the current form. Generally, there are two possible ways to solve the problem. First, by mapping the transmitting network nodes to the *seeds* in the Voronoi diagram, the PED-based method can be evolved to fit more general network scenarios. The Voronoi diagram is a special kind of plane decomposition determined by the distances to a specified discrete set of objects, which are usually termed as the *seeds*. Within a Voronoi diagram, each seed solely occupies a *Voronoi cell* consisting of all points closer to the seed than to any other ones. It is easy to find out that, the correlation between a seed and its Voronoi cell is quite similar to the one between a transmitting network node and its exclusive region. Therefore, the Voronoi diagram has been widely used in the performance analyses of wireless networks, e.g., for more realistically modeling the distribution of the base stations in cellular networks. By applying similar ideas, we are currently working on the re-definition and calculation of the equivalent PED when each transmitting node's exclusive region is modeled by the Voronoi cell. With the new results, the PED-based approach can still be applied over the irregular network area without the constraint of nodes density and traffic intensity. Second, considering we already obtained the bound performance in this paper, it is always possible to establish connections between the bound and the general cases by introducing a variable coefficient. For example, with the same expression shown in (1), the pathloss only scenarios can be presented with the fading coefficient $h_x = 1$, while the more general fading included scenarios could be illustrated with h_x as a random variable. Based on this idea, we are comparing the result obtained in this paper with the accumulated interference power's distribution when the

network nodes follow a Poisson point process. Hopefully, we may able to summarize some useful results with the help of Stochastic Geometry, and provide easy to be used tools for obtaining not only performance bounds but also the probability distributions.

As described in the system model, due to the analysis complexity and the requirement for arranging the concurrently communicating D2D node pairs, the power attenuation during the signal transmission only considered the pathloss effect in this paper. The main difficulty for moving from the pathloss model to the more complicated fading model is that, the coefficient $h_{\mathrm{d}S}$ in equation (2) will become a random variable for all the exclusive regions, which means the area integral in (2) may not able to be calculated directly. For this issue, we are currently working on obtaining the moments of $I_{\mathrm{ACC}}(y)$ first. The experience for handling the area integral in different cases, when the PED-based method was firstly studied, can be reused here, however, the newly added random variable $h_{\mathrm{d}S}$ greatly increased the complexity. In some cases, the approximation or numerical method just become necessary. Some results have already been obtained for the situation when the channel fading can be described by the Rayleigh model, which makes the received signal power follow the exponential distribution and simplifies the related derivations. By following the similar method, we will also work on other more general fading models in the near future.

IX. Conclusions

In this paper, with the help of our recently proposed PED-based interference analysis method, we have derived the guard distances of BS, CUE, and DUE for enabling multiple D2D communications in a sector-partitioned cell by utilizing the identical radio resource designated for the uplink cellular transmission. In addition, we have also obtained the bounds and the expectation of the maximum throughput improvement provided by D2D communications in a single cell. Beside the validation of the PED-based method's accuracy, the major results of this paper can be summarized into two points:

- First, for the underlaying D2D communications, more complicated sector-based resource allocation scheme leads to a higher throughput improvement, but this improvement will not be obvious when the BS's guard distance G_{B} is relatively small.
- Second, a larger sector number could provide higher performance gains, but the increment is decreased with the increasing sector number.

We believe this work will provide useful insights for the design and optimization of more efficient D2D communications in cellular networks. Using the similar method, we plan to study the performance of D2D communications under more realistic fading channels, which will introduce randomness on the ERs coexisted in the network, and lead to some new results presented in a probabilistic way. Moreover, the scenario that the downlink radio resources are reused will also be investigated in the near future.

References

[1] M. Ni, L. Zheng, F. Tong, J. Pan, and L. Cai, "A geometrical-based throughput bound analysis for device-to-device communications in cellular networks," *IEEE J. Sel. Areas Commun.*, vol. 33, no. 1, pp. 100–110, Jan. 2015.

[2] M. Haenggi and R. K. Ganti, "Interference in large wireless networks," *Found. Trends Netw.*, vol. 3, no. 2, pp. 127–248, 2009.

[3] M. Ni, J. Pan, and L. Cai, "Power emission density-based interference analysis for random wireless networks," in *Proc. IEEE ICC*, 2014, pp. 440–445.

[4] P. Jänis *et al.*, "Device-to-device communication underlaying cellular communications systems," *Int. J. Commun., Netw. Syst. Sci.*, vol. 2, no. 3, pp. 169–178, 2009.

[5] C.-H. Yu, K. Doppler, C. B. Ribeiro, and O. Tirkkonen, "Resource sharing optimization for device-to-device communication underlaying cellular networks," *IEEE Trans. Wireless Commun.*, vol. 10, no. 8, pp. 2752–2763, Aug. 2011.

[6] H. S. Chae, J. Gu, B.-G. Choi, and M. Chung, "Radio resource allocation scheme for device-to-device communication in cellular networks using fractional frequency reuse," in *Proc. IEEE APCC*, 2011, pp. 58–62.

[7] P. Phunchongharn, E. Hossain, and D. Kim, "Resource allocation for device-to-device communications underlaying LTE-advanced networks," *IEEE Wireless Commun. Mag.*, vol. 20, no. 4, pp. 91–100, Aug. 2013.

[8] L. Song, D. Niyato, Z. Han, and E. Hossain, "Game-theoretic resource allocation methods for device-to-device communication," *IEEE Wireless Commun. Mag.*, vol. 21, no. 3, pp. 136–144, Jun. 2014.

[9] Y. Cheng, H. Han, and X. Lin, "Device-to-device communication in CDMA-based cellular systems—Uplink capacity analysis," in *Proc. IEEE Commun. Softw. Netw.*, 2011, pp. 430–434.

[10] H. Min, J. Lee, S. Park, and D. Hong, "Capacity enhancement using an interference limited area for device-to-device uplink underlaying cellular networks," *IEEE Trans. Wireless Commun.*, vol. 10, no. 12, pp. 3995–4000, Dec. 2011.

[11] Z. Liu, T. Peng, Q. Lu, and W. Wang, "Transmission capacity of D2D communication under heterogeneous networks with dual bands," in *Proc. IEEE CROWNCOM*, 2012, pp. 169–174.

[12] B. H. Jung, N.-O. Song, and D. K. Sung, "A network-assisted user-centric wifi-offloading model for maximizing per-user throughput in a heterogeneous network," *IEEE Trans. Veh. Technol.*, vol. 63, no. 4, pp. 1940–1945, May 2014.

[13] D. Niyato, P. Wang, and D. I. Kim, "Performance modeling and analysis of heterogeneous machine type communications," *IEEE Trans. Wireless Commun.*, vol. 13, no. 5, pp. 2836–2849, May 2014.

[14] P. Gupta and P. R. Kumar, "The capacity of wireless networks," *IEEE Trans. Inf. Theory*, vol. 46, no. 2, pp. 388–404, Mar. 2000.

[15] R. P. Feynman, R. B. Leighton, and M. Sands, *The Feynman Lectures on Physics*. Reading, MA, USA: Addison-Wesley, Aug. 2005.

[16] T. Rappaport, *Wireless Communications: Principles and Practice*. Englewood Cliffs, NJ, USA: Prentice-Hall, 2001.

[17] F. Xue and P. R. Kumar, "Scaling laws for Ad Hoc wireless networks: An information theoretic approach," *Found. Trends Netw.*, vol. 1, no. 2, pp. 145–270, Jul. 2006.

[18] K. Stephenson, "Circle packing: A mathematical tale," *Notices Amer. Math. Soc.*, vol. 50, pp. 1376–1388, 2003.

[19] T. Yang, G. Mao, and W. Zhang, "Connectivity of large-scale CSMA networks," *IEEE Trans. Wireless Commun.*, vol. 11, no. 6, pp. 2266–2275, Jun. 2012.

[20] L. Cai, L. Cai, X. Shen, J. W. Mark, and Q. Zhang, "MAC protocol design and optimization for multi-hop ultra-wideband networks," *IEEE Trans. Wireless Commun.*, vol. 8, no. 8, pp. 4056–4065, Aug. 2009.

[21] Wolfram MathWorld, Hypergeometric Function. [Online]. Available: http://mathworld.wolfram.com/HypergeometricFunction.html

[22] "Selection Procedures for the Choice of Radio Transmission Technologies of the UMTS," Tech. Rep. TR 30.03U V3.2.0, 1998.

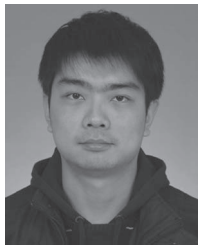

Minming Ni (S'08–M'13) received the B.S. and Ph.D. degrees from Beijing Jiaotong University, Beijing, China, in 2006 and 2013, respectively. He worked as a Visiting Student at McMaster University, Hamilton, ON, Canada, from 2010 to 2011, and also as a Postdoctoral Research Fellow at the University of Victoria, Victoria, BC, Canada, from 2013 to 2014. His research interests include wireless network modeling and performance analysis, vehicular ad hoc networks, and device-to-device communications.

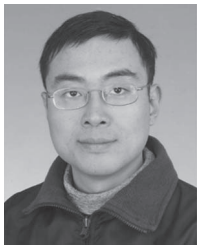

Jianping Pan (S'96–M'98–SM'08) received the B.S. and Ph.D. degrees in computer science from Southeast University, Nanjing, Jiangsu, China, and did his postdoctoral research at the University of Waterloo, Waterloo, Ontario, Canada. He also worked at Fujitsu Labs and NTT Labs. He is currently an Associate Professor of computer science at the University of Victoria, Victoria, BC, Canada. His area of specialization is computer networks and distributed systems, and his current research interests include protocols for advanced networking, performance analysis of networked systems, and applied network security. He received the IEICE Best Paper Award in 2009, the Telecommunications Advancement Foundation's Telesys Award in 2010, the WCSP 2011 Best Paper Award, the IEEE Globecom 2011 Best Paper Award, the JSPS Invitation Fellowship in 2012, and the IEEE ICC 2013 Best Paper Award, and has been serving on the technical program committees of major computer communications and networking conferences including IEEE INFOCOM, ICC, Globecom, WCNC, and CCNC. He was the Ad Hoc and Sensor Networking Symposium Co-Chair of IEEE Globecom 2012 and an Associate Editor of IEEE TRANSACTIONS ON VEHICULAR TECHNOLOGY. He is a senior member of the ACM.

Lin Cai (S'00–M'06–SM'10) received M.A.Sc. and Ph.D. degrees in electrical and computer engineering from the University of Waterloo, Waterloo, ON, Canada, in 2002 and 2005, respectively. Since 2005, she has been an Assistant Professor and then an Associate Professor with the Department of Electrical and Computer Engineering, University of Victoria, Victoria, BC, Canada. She has been an Associate Editor for IEEE TRANSACTIONS ON WIRELESS COMMUNICATIONS, IEEE TRANSACTIONS ON VEHICULAR TECHNOLOGY, *EURASIP Journal on Wireless Communications and Networking*, the *International Journal of Sensor Networks*, and the *Journal of Communications and Networks*. Her research interests include wireless communications and networking, with a focus on network protocol design and control strategy supporting emerging applications in ubiquitous networks.